Revised Manuscript
Click here to view linked References
https://doi.org/10.1016/j.jhazmat.2022.129698
This is the Pre-Published Version.

**Title:** Dietary exposure to polystyrene nanoplastics impairs fasting-induced lipolysis in adipose tissue from high-fat diet fed mice.

**Author:** Ho Ting Shiu[1,2,#], Xiaohan Pan[1#], Qing Liu[1], KeKao Long[3], Kenneth King Yip Cheng[3], Ben Chi-Bun Ko[1], James Kar-Hei Fang[1,4], Yuyan Zhu[1,4,5,*]

**Affiliation:**

From the [1]Department of AppliedBiology and Chemical Technology, [3] Department of Health Technology and Informatics, [4] Research Institute for Future Food, [5] Research Centre for Chinese Medicine Innovation, The Hong Kong Polytechnic University, Hung Hom, Kowloon, Hong Kong, China

[2] current address: Department of Pharmacology and Pharmacy, The University of Hong Kong, Pokfulam, Hong Kong, China

# Xiaohan Pan and Ho Ting Shiu contributed equally to this work

***** Corresponding to yuyan.zhu@polyu.edu.hk

- **Abstract**

The health concerns of microplastics (MPs) and nanoplastics (NPs) surge, but the key indicators to evaluate the adverse risks of MPs/NPs are elusive. Recently, MPs/Ps were found to disturb glucose and lipid metabolism in rodents, suggesting that MPs/NPs may play a role in obesity progression. In this study, we firstly demonstrated that the distribution of fluorescent polystyrene nanoplastics (nPS, 60 nm) white adipose tissue (WAT) of mice. Furthermore, nPS could traffic across adipocytes in vitro and reduced lipolysis under β-adrenergic stimulation in adipocytes *in vitro* and *ex vivo*. Consistently, chronic oral exposure to nPS at the dietary exposure relevant concentrations (3 and 223 μg/kg body weight) impaired fasting-induced lipid mobilization in obese mice and subsequently contributed to larger adipocyte size in the



© 2022. This manuscript version is made available under the CC-BY-NC-ND 4.0 license http://creativecommons.org/licenses/by-nc-nd/4.0/

subcutaneous WAT. In addition, the chronic exposure of nPS induced macrophage infiltration in the small intestine and increased lipid accumulation in the liver, accelerating the disruption of systemic metabolism. Collectively, our findings highlight the potential obesogenic role of nPS via diminishing lipid mobilization in WAT of obese mice and suggest that lipolysis relevant parameters may be used for evaluating the adverse effect of MPs/NPs in clinics.

**Key words**: nanoplastics, obesity, adipose tissue, lipolysis

**Highlights**

- Nano-sized PS accumulated in white adipose tissue in mice.
- nPS at the physiological relevant level showed little effect on adipogenesis
- nPS at the diet-relevant level suppressed lipolysis in high-fat diet fed mice
- nPS induced inflammation in the small intestine.
- nPS enhanced fat accumulation in the liver in high-fat fed mice.

**Abbreviations:**

| | |
|---|---|
| microplastics | MP |
| nanoplastics | NP |
| polystyrene nanoplastics | nPS |
| white adipose tissue | WAT |
| high-fat diet | HFD |
| intraperitoneal glucose tolerance test | IPGTT |
| immunohistochemistry | IHC |
| triacylglyceride | TG |

| | |
|---|---|
| free fatty acid | FFA |
| fatty acid synthase | FAS |
| diacylglycerol acyltransferase | DGAT |
| adipose triglyceride lipase | ATGL |
| hormone-sensitive lipase | HSL |
| monoglyceride lipase | MGL |
| epididymal WAT | epiWAT |
| inguinal WAT | ingWAT |

- **Graphical abstract**

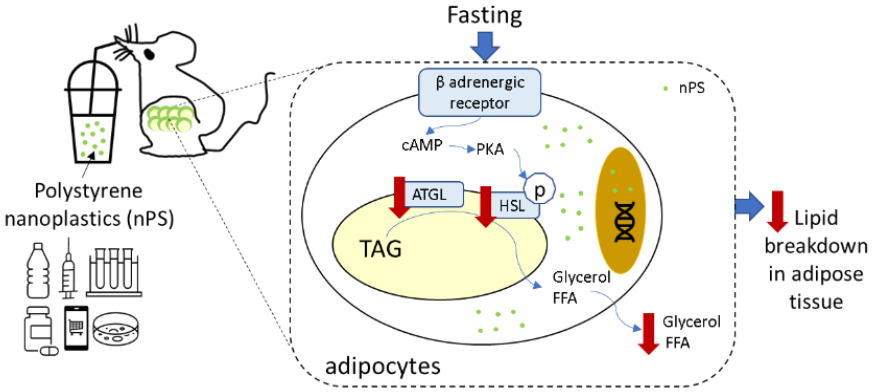


## 1. Introduction:

The fast-growing of plastic pollution has raised awareness among the globe and many policies have been implemented to slow down the drastically increasing plastic usage and plastic pollution (1). About 8.3 billion metric tons of plastics have been accumulated in the environment by 2017 (2), and the annual production of plastics increased from 225 million tonnes in 2004 to 368 million tonnes in 2019 globally (3). Recently, the outbreak of COVID-19 pandemic has disrupted this progress. With the mandatory requirement of wearing facemasks and the increased use of personal protective equipment, an estimation of 1.6 million

tonnes of plastic waste are made every day worldwide since the outbreak of COVID-19 (4,5). The half-life of plastics ranges from 4.6 (e.g. plastic bags) to 5000 years (e.g. pipes) on land, while microscale and nanoscale plastic particles are continuously released during the degradation process (6). Consequently, the environmental and health concerns of plastics arise overtime.

Microplastics (MPs, 1 μm - 5 mm in size) (7) and nanoplastics (NPs, 1 - 1000 nm in size) (8-10) are unwanted particles that result from the manufacturing and degradation of plastic objects. We are exposed to MPs/NPs mainly through indoor air inhalation (11,12), drinking water (13) and food-chain ingestion (11). NPs can be fragmented from MPs (14), and are detected in several organs such as the intestine, liver, kidney, heart and even lymph nodes of rodents (15). Besides their wide distribution, smaller-sized NPs could be taken up more efficiently than MPs (16). In addition, NPs may attach more easily than MPs to organic chemicals/molecules due to their larger surface area (17). A recent study has discovered plastic particles of various polymer types in human blood, indicating that plastic particles can circulate in the human body and can reach various organs in the human body (18). Therefore, the evaluation of the potential health risks of NPs is necessary.

The clinical evidence about the health risks of MPs/NPs is still lacking. However, an increasing number of animal studies have raised the health concerns of the potential harmful effects of MPs/NPs. In aquatic organisms, the toxicity of MPs/NPs (19) has been reported mainly in the digestive (20-22), reproductive (23,24), nervous (25,26) and immune systems (27,28), as well as the embryo development (29,30). In laboratory rodents, the health repercussions of MPs/NPs seem to be relatively mild (19,31-34). As reviewed in (35-37), previous rodent studies have revealed that MPs/NPs caused inflammation in the respiratory system (38,39), damaged the

intestinal barrier function and altered microbiota (40,41), stimulated oxidative stress and subsequently disturbed glucose and lipid metabolism in the liver (41,42), impaired spermatogenesis and its associated reproductive hormone function (43,44). However, the effects of NPs on anxiety and cognition in rodents are lack of consistency (31-33). Furthermore, compared to MPs, smaller-sized NPs generally presented longer retention time in aquatic organisms (45,46) and more severe damage in the reproductive and nervous systems (35), but with less disturbance in the liver (25,47).

There are only a few studies investigated the role of NPs in lipid metabolism and adiposity, and the effect is inconclusive yet. In chow diet fed lean mice, orally exposure to NPs was reported to reduce lipid accumulation in the liver and adipose tissue in ICR mice (48). In contrast, same dosage and size of NPs treatment was found to increase adiposity in male C57BL/6 mice (49). Meanwhile, orally exposure to higher dosages (5 and 15 mg/kg body weight) of NPs significantly increased hepatic lipids and serum glucose level with little effect in body weight (50). In high fat diet (HFD) fed obese mice, NPs treatment via i.v. injection accelerated lipid accumulation and fibrosis in the liver as well as increased body weight (42). These above data suggested that acute NPs exposure could disturb systemic lipid metabolism and adiposity, however, the underlying mechanism remains elusive (37).

Herein, we evaluated the distribution and physiological effects of dietary exposed polystyrene-nanoplastics (nPS) at the cellular, tissue, and organismal levels. Polystyrene was employed as a representative NP due to its commonality in the production of carryout containers (37) and plastic wastes (51). The dosage of nPS we used *in vitro* is relevant to the plastic particle level in human blood (18), and that *in vivo* is relevant to dietary exposure level (11,52,53). Thus, our results reflect the health risks of nPS we may be facing currently. Our findings revealed

the preferential accumulation of nPS in white adipose tissue (WAT) and demonstrated for the first time that nPS impaired lipid mobilization upon lipolytic stimulation in adipose tissue. These data suggested a potential obesogenic role of nPS.

## 2. Materials and methods:

### 2.1 Nanoparticle and Chemicals.

Polystyrene nanoparticles (nPS, Cat No.17149, Polysciences, Warrington, PA, USA). nPS particles ($3.64 \times 10^{14}$ particles/mL) were suspended in milliQ water as the stock. nPS were analysed with Raman spectroscopy (Wotton-under Edge, England) (54) and NanoSight (Spectris, UK). Other Detailed chemicals and reagents are in the Supplementary material (Supplementary table 1-3).

### 2.2 Raman microspectroscopy of nPS.

The nPS particles were characterized with Raman spectroscopy using a Renishaw inVia confocal Raman microscope (Wotton-under Edge, UK) equipped with a Leica 50x objective (Wetzlar, Germany) and a 785 nm excitation laser (300 mW output power). The nPS were deposited on a flat surface of aluminium to form a continuous particle film, from which a Raman spectrum was acquired for 5 s using 10% laser power in the wavenumber range of 676 – 1767 $cm^{-1}$. The Raman microscope was calibrated using the vibrational band at 520 $cm^{-1}$ of a silicon reference (54). The spectrum of nPS was compared against the spectra of standard plastics provided in the Renishaw Polymeric Materials Database.

### 2.3 Animals and Treatments.

Three-week-old male C57BL/6J mice were purchased from The Chinese University of Hong Kong (Hong Kong) and housed in the Centralized Animal Facilities in The Hong Kong

Polytechnic University on a 12/12 h light/dark cycle at 22–25 °C. Food and water were provided *ad libitum*. These mice were randomly assigned into three groups (n = 5) to receive drinking water with different concentrations of nPS supplemented (corresponding to 0, 2.8, 223 μg/day/kg body weight) for 8 consecutive weeks, starting from their age at 5 weeks old (Figure 5A). The low-nPS and high-nPS concentrations correspond to the daily consumption of $1.44 \times 10^9$ and $9.74 \times 10^{10}$ particles/mouse/day, respectively. All three groups of mice were given HFD (Cat No.D12492, Research diets Inc., New Brunswick, NJ, USA) during the 8 weeks' experimental period. The major ingredients in the HFD are lard (31.66% in weight), casein (25.84% in weight) and maltodextrin 10 (16.15% in weight). The fat content contributes to 60% of total calorie in the diet. Experimental procedures were approved by the Animal Subjects Ethics Sub-Committee. After the mice were sacrificed, the tissue and serum samples were collected for further analysis.

**2.4 Fasting blood glucose level and intraperitoneal glucose tolerance test (IPGTT).**

Mice were fasted overnight for 12 hours before performing the IPGTT, as described previously (55). The blood was drawn from tail vein and the glucose level was measured at 0, 15, 30, 45, 60, 120 minutes after injecting glucose solution at the dosage of 2 g/kg bodyweight intraperitoneally.

**2.5 IVIS Imaging.**

Full body and tissue distribution of nPS was visualized using the Perkin-Elmer IVIS Imaging System (PerkinElmer, Waltham, MA, USA). Briefly, nPS particles were suspended in water and administrated to 9-week-old C57BL/6J female mice via oral gavage for four consecutive days at a concentration of 0 or 500 μg/day/mouse. During these four days, mice (n = 2) were assigned to either chow or HFD *ad libitum*. Two hours after the fourth dosage, mice were

anesthetized by ketamine/xylazine and shaved before full body imaging. During imaging process, the mice received isoflurane gas anesthesia. Fluorescent images of both dorsal and ventral sides of the mice were taken under λex / λem at 440 nm / 520 nm, which is the closest wavelength to the fluorescent spectrum of the nPS administrated. A binning factor of "8" and the exposure time of "4 seconds" were used. The region of interest (ROI) of the control mice, which did not receive any fluorescent nPS administration, was selected and its fluorescent signal was calculated as the background to generate the background-subtracted image for the treatment group. The fluorescent signal intensity was expressed in radiance (Figure 2A), with red as strong signals and blue as weak signals. Afterwards, blood was drawn by cardiac puncture and the tissues were taken out for IVIS imaging on a black colour paper to minimize the background fluorescence. A binning factor of "4" and the exposure time of "3 seconds" were set to take pictures under λex / λem at 440 nm / 520 nm. The fluorescent signal intensity was expressed in radiant efficiency, with yellow to indicate strong fluorescent signals and dark-red as weak signals (Figure 2A). Living Image® software (PerkinElmer, USA) was used for data analysis after the pictures were captured.

**2.6 Histological analysis.**

WAT tissues from the experimental mice were cryosectioned in 20-μm thickness under -30 °C. Adipocyte diameters were quantified by Adiposoft software. Liver tissues were cryosectioned in 10-μm, followed by H&E staining. The small intestine samples were processed with gut bundle method as described before (56), followed by paraformaldehyde fixation and paraffin embedding. The 5-μm sections were used for F4/80 immunohistochemistry (IHC) and hematoxylin nuclei staining. To quantify the number of macrophages/villus, we randomly

selected 5 areas/section with the optical microscope (Olympus CKX41, Tokyo, Japan). The number of F4/80 positive cells per villus was calculated.

**2.7 Intracellular visualization of nPS.**

For visualization of nPS-fluorescent signal, cells were fixed with 4% paraformaldehyde and the nucleus was stained with Hoechst 33342. Images were taken with a Leica TCS SPE Confocal Microscope (Leica, Germany).

**2.8 Adipocyte Cell Culture and Analysis.**

The 3T3-L1 murine preadipocytes (ATCC, Manassas, VA, USA) were maintained and differentiated as described previously (57). nPS were added in the culture medium to achieve the concentrations of $10^5$ and $10^{10}$ particles/ml during the differentiation period from Day 0 to Day 6. Afterwards, the cells were subjected to Oil Red O staining, qPCR analysis, or confocal imaging.

**2.9 nPS uptake analysis.**

3T3-L1 preadipocytes and mature adipocytes were seeded in a 96-well black plate and treated with nPS under serum free medium, incubated at 37 °C with 5% $CO_2$. Additionally, preadipocytes cultured in the presence or absence of nPS ($10^{10}$ particles/ml) were put on ice for passive internalization examination. After that, the cells were washed with PBS three times to remove any non-internalized nPS. The intracellular nPS-fluorescent signal was quantified by a microplate reader (Thermo Scientific, Waltham, MA, USA) at Ex/Em of 441/486 nm.

**2.10 Lipolysis Assay**.

Lipolysis analysis was performed as described before (58). Briefly, for *in vitro* lipolysis, 3T3-L1 cells were differentiated for 6-8 days in the presence or absence of nPS ($10^{10}$ particles/ml), and then adipocytes were incubated in a glucose medium containing 2% fatty-acid-free BSA with or without isoproterenol (10 μM). Similarly, for *ex vivo* lipolysis, mouse epididymal WAT was minced and cultured in low glucose DMEM containing 2% fatty-acid-free BSA in the presence or absence of nPS ($10^{10}$ particles/ml) for 1 hour. Then, 10 μM isoproterenol or vehicle was added into the medium for 6 hours. The glycerol in the culture medium was quantified with an associated kit (Nanjing Jiancheng, China) according to the manufacturer's protocol. Total protein in cells/tissues was quantified with BCA method for normalization.

### 2.11 RNA isolation and Quantitative Real‑time PCR.

Total RNA was extracted from the indicated tissues after homogenizing by a tissue homogenizer together with Trizol. The cDNA was synthesized with PrimeScript RT Master Mix (Takara, Japan). Applied Biosystems™ QuantStudio™ 7 Flex Real-Time PCR System (Waltham, MA, USA) was used with TB Green® Premix Ex Taq™ (Tli RNase H Plus) (Takara, Japan) to quantify gene expression as described earlier (57). The primers are listed in supplementary table 1. Expression fold change was calculated using the ΔΔCT method using Ppia as the housekeeping gene.

### 2.12 Total Protein Extraction and Immunoblotting.

Total protein was extracted from WAT and immunoblotting was performed as described before (57). β-actin was used as the internal control. The primary antibodies are listed in the supplementary table 2.

### 2.13 Measurement of Liver Triacylglyceride (TAG) and serum free fatty acid (FFA).

Liver samples were homogenized with 100% ethanol by a tissue homogenizer. The samples were centrifuged, and supernatant was collected for TAG measurement using a TAG assay kit (cat. no. A110-1-1, Nanjing Jiancheng, China). The serum free fatty acid (FFA) level was measured using an FFA kit (cat. no. A042-2-1, Nanjing Jiancheng, China).

### 2.14 Statistical Analysis.

All data are shown as means ± SEM. Two tailed student's T-test was used to calculate the statistical difference between two groups. One-way ANOVA with Tukey post-hoc test was applied to compare among three groups. All statistical analyses were performed using Prism 9 (GraphPad, San Diego, CA). $P < 0.05$ was considered statistically significant.

## 3. Results and Discussion

### 3.1 Characteristics of nano-PS

For easier tracking of the distribution of NPs, fluorescent nPS were employed and their fluorescent signal can be clearly visualized under fluorescent microscopy (Figure 1A). With the help of Raman microspectroscopy, the spectrum of nPS used in this study was compared against the spectra of standard plastics provided in the Renishaw Polymeric Materials Database, and was confirmed to be PS according to the characteristic peaks at 1001 $cm^{-1}$, 1031 $cm^{-1}$ and 1603 $cm^{-1}$ (Figure 1B). In addition, the mean diameter of nPS under water suspension was 63.2 ± 10.6 nm (Figure 1C), and the sharp peak (Figure 1C) suggested that the size of nPS we used was relatively uniform. In addition, the fluorescence leakage from the our nPS particles in the gastric juice (pH = 2) was less than 1% over the period of 24 hours' incubation (Figure S1), suggesting the fluorescence leakage may be negligible.

### 3.2 nPS preferentially accumulate in white adipose tissue in mice.

Nanoplastics have been detected in various organs, including the liver, lungs, kidney, heart, lymph nodes, spleen, brain in different rodents (37), as well as in the offsprings of NP exposed-rats (59). In humans, the presence of MPs in the placenta (60), colon (60) and feces (53) has also been reported. However, the accumulation of NPs in adipose tissue is understudied. To examine the body distribution of nPS in mice, we employed IVIS imaging system and observed that dietary nPS particles were widely distributed in the main bodies of mice that were fed with either HFD or chow diet (Figure 2A). The stomach and WAT at both perigonadal (visceral) and inguinal (subcutaneous) sites showed strong fluorescent-nPS signal (Figure 2B), but such strong signal was undetectable in the major organs, including the liver, kidney, pancreas, and spleen (Figure 2B). Interestingly, we did not observe the fluorescent-nPS signal in the lipid droplets of adipocytes (Figure 2C).

Interestingly, during the preparation of this manuscript, Dr. Q. Hui's group reported that nPS via tail vain injection at a high dosage (about 25 times higher than the concentration used here) could reach various organs, with the strongest nPS-fluorescent signal found in the WAT, liver and lungs (50). These data supported our finding that nPS could reach the WAT. Whether WAT works as an nPS "reservoir" in the body needs further investigation. Collectively, these data illustrated the co-localization of dietary nPS and WAT, suggesting a potential impact of nPS on the adipose tissue function *in vivo*.

### 3.3 nPS shuttles across adipocytes *in vitro* but have little effect on adipogenesis at the physiological relevant dosage.

nPS-fluorescent signal was observed in the mice's WAT (Figures 2B, C), thus, we employed murine 3T3-L1 preadipocyte cell line to further evaluate the mobilization of nPS in adipocytes. Recently, 1.6 μg/ml of plastic particles were quantified in serum from several clinical samples

(18), and this concentration corresponds to about $10^{10}$ particles/ml of 60 nm-sized nPS. We found that nPS ($10^{10}$ particles/ml) in the culture medium efficiently internalized into both preadipocytes and adipocytes within 4-8 hours, and with higher accumulation level in preadipocytes than in mature adipocytes (Figure 3A). Interestingly, preadipocytes on ice presented fluorescent-nPS signal within 8 hours of incubation (Figure 3A), suggesting that nPS could passively enter preadipocytes. Consistently, nPS was reported previously to be able to passively enter model cell membranes and rat basophilic leukemia cells (61). For the intracellular distribution of nPS, the 3D imaging at a series of focal planes by confocal microscopy revealed that the nPS particles were mainly distributed in the cytoplasm (Figure 3B) and were able to enter the cell nucleus (white arrow pointing to the intranuclear green-nPS signal in Figures 3B), but not in the lipid droplets of adipocytes (Figure S2). 60 nm-sized nPS particles were also detected in the nuclei of Caco-2 cells previously (62), but not in rat basophilic leukemia (RBL-2H3) cells (63), suggesting their intracellular distribution varied among different cells. After the adipocytes were loaded with nPS during adipogenesis, we observed that intracellular nPS-fluorescent signal reduced significantly after lipolysis (Figure 3C). It suggested a possible excretion of nPS from adipocytes, which may be via exocytosis/penetration as similar to that in rat basophilic leukemia (RBL-2H3) cells (61). Collectively, we demonstrated that nPS could both passively and actively internalize into the cytoplasm and nucleus in preadipocytes and adipocytes, and that nPS may exit adipocytes during lipolysis. However, in the lipid-droplet containing adipocytes, how nPS shuttles across the membranes needs further study.

The ability of nPS to enter the cell nuclei brings a serious health concern, since cell division and transcriptional regulation occur in the cell nuclei. Whether nPS internalization could influence adipocyte function remains unclear. The dominant role of adipocytes is for energy

storage, and thus, adipogenesis and lipogenesis are the main bioprocesses in adipocytes. In 3T3-L1, nPS treatment at circulation relevant dosages of $10^5$ or $10^{10}$ particles/ml throughout the whole period of adipogenesis had little effect on lipid accumulation (Figure 3D) or the mRNA levels of genes involved in lipid production [fatty acid synthase (FAS), diacylglycerol acyltransferase 1 and 2 (DGAT1, DGAT2)] (Figure 3E). These findings suggested that nPS with up to about 0.8 μg/ml dosages ($10^{10}$ particles/ml) had minimal influence on adipogenesis or lipogenesis *in vitro*. In contrast, plastic particles with larger size (400 nm) and higher concentration (1.2 - 2.4 mg/ml) showed the pro-adipogenic effect in bone marrow stem cells (64). The controversy is mainly due to the difference in concentration. Dr. Rotchell's team have compared 168 *in vitro* studies and concluded that higher concentration of NPs have stronger affect in adipocytes (65). Since the dosage we used here is relevant to the plastic particle level in human blood, thus, NPs may not show clear pro-adipogenic effect currently. However, with the inevitable accumulation trend of environmental plastics, we could perspeculate a potential obesogenic role of NP at high exposure concentration in the future.

### 3.4 nPS treatment impairs glycerol release upon lipolytic stimulation in adipocytes *in vitro*.

Lipid mobilization in adipocytes plays an important role in regulating systemic energy balance (66), and lipolysis is a process to break down TAG for providing energy to other organs (67). Three neutral lipases, adipose triglyceride lipase (ATGL), hormone-sensitive lipase (HSL) and monoglyceride lipase (MGL), are responsible for sequential hydrolysis of TAG to glycerol and fatty acids (66). Pro-lipolytic hormones mediate the phosphorylation of HSL and cofactors (like perilipin), and subsequently the intracellular relocation of the lipases for TAG hydrolysis (67). It was reported that nanoparticles induced autophagy in several cells (68,69), while lipid degradation in adipocytes could be mediated by autophagy (67). Therefore, we hypothesized

that internalized nPS in the adipocytes may affect lipid mobilization. The lipolysis is low in the fed state (basal state), but can be induced upon energy demanding (e.g. fasting or hormone stimulation, termed as stimulated state, Figure 4A). We quantified glycerol, the end product of lipolysis, under basal and stimulated (isoproterenol, which is a β adrenergic receptor agonist) conditions, respectively. Surprisingly, nPS treatment lowered isoproterenol-induced free glycerol in the medium (Figure 4B), without affecting the basal lipolysis level. To bridge the *in vitro* and *in vivo* gap, we employed epididymal WAT (epiWAT) from male mice (8 weeks old) as the *ex vivo* model. Consistently, acute treatment of nPS in cultured WAT also tended to reduce glycerol level in the medium under isoproterenol's stimulation (Figure 4C, $p = 0.053$). These data demonstrated that nPS may impair β adrenergic receptor-mediated lipolysis in adipose tissue *in vitro*. It is well known that β adrenergic receptor-mediated lipolysis is impaired in obese patients with lower levels of adenylyl cyclase activity (70), therefore, we further investigated the role of nPS in lipolysis in obese mice *in vivo*.

**3.5 Chronic oral exposure to nPS impairs fasting-induced lipolysis in obese mice.**

HFD fed C57BL/6J male mice were given drinking water supplemented with different doses of nPS (Figure 5A). The exposure dosages of MPs/NPs vary significantly according to geographic location and lifestyle in reality, thus the two concentrations of nPS we used in this study were chosen to represent low- and high-exposure scenarios: The low concentration was calculated based on the nanoplastic exposure level from one cup of tea (52) as well as the dose conversion between mice and human (12.3:1) (71). The high concentration was based on the estimated exposure level in US (11,53) and the dosage commonly used in many other research papers (40,48,72). The treatment stage covered the period from adolescence to adult years (from 5 weeks to 13 weeks), which provides an insight into the nPS' effect to the young generation with the drastically increase in nPS exposure in recent years.

During the 8 weeks treatment period, neither the body weight, food intake, nor water intake of the mice were significantly affected by dietary nPS at the tested dosages (Figures 5B-D). Consistently, nPS at the tested dosages had little effect on the weight of different organs (Figure 5E-G) or HFD-induced glucose intolerance (Figure 5H, I). Previous studies had reported adverse effects of nPS on glucose metabolism and hepatic fibrosis (42,50), which were not detected in our study. The possible reasons for the inconsistent phenotypes could be largely due to the differences in exposure concentration and size of the particles, mouse gender and diet-induced metabolic model.

Previously, we demonstrated the impaired stimulated-lipolysis in both *in vitro* adipocytes (Figure 4B) and *ex vivo* WAT models (Figure 4C). Consistently, we found that H-nPS-exposed mice had significantly lower serum FFAs level after overnight fasting (Figure 6A), while these serum FFAs were predominantly released from WAT. Furthermore, we found that the inguinal WAT (ingWAT) from the nPS-exposed mice had bigger adipocytes than the control mice (Figure 6B), which suggested an upregulated TAG synthesis or a downregulated lipolysis in the WAT. Since the mRNA levels of genes involved in lipid synthesis in WAT were either unaltered or reduced (Figure 6C), the enlarged size of adipocytes was not likely to have attributed to lipogenesis in the nPS-treated mice. Then, we examined the lipolysis associated proteins in WAT. Consistent with our *in vitro* data, nPS treatment significantly reduced the protein levels of lipolytic enzymes (ATGL, HSL and phosphorylated-HSL$^{s660}$) in epiWAT (Figure 6D). Adipocytes from obese humans showed lower lipolysis under hormone-stimulation and decreased levels of HSL than that from lean individuals (73), while ATGL and HSL are responsible for sequential hydrolysis of TAG to glycerol and fatty acids (66). Collectively, nPS impaired fasting-stimulated lipolysis in WAT and contributed to the larger

size of adipocytes in WAT, which will potentially promote obesity development. These findings suggested that the lipolysis relevant parameters may be used for evaluating the adverse effect of MPs/NPs in clinics. To our knowledge, the role of MPs/NPs on lipolysis has been ignored in the field.

Prior studies mainly used chow diet fed lean mice, in which the effects of NPs in adiposity were controversial (48,49). Oral exposure of NPs (500 nm at 200 μg/kg) for 5 weeks lowered body weight and lipid level in adipose tissue (48), while another group showed polystyrene bead ingestion (500 nm at 3.6 μg/day/mouse) for 12 weeks promoted adiposity and cardiometabolic disease (49). Thus, the obesogenic role of NPs in lean mice may not be that significant. Compared with regular chow diet, HFD feeding induces a feature of permeable gut barrier in animals (74) and humans (75), which may facilitate the absorption of dietary NPs. Furthermore, HFD feeding was reported to accelerate the adverse effects of pollutants, like glucose intolerance, lipid metabolic disorder and liver injury (76), thus, HFD may amplify the health risks of NPs. In our study, we employed HFD fed mice and revealed the anti-lipid mobilization role of nPS. Further investigating on the interaction of HFD and nPS could reveal whether we could minimize the adverse effect of MPs/NPs by manipulating our diet.

**3.6 Chronic oral exposure to nPS accelerates lipid accumulation in the liver.**

It was widely reported that MPs/NPs induced inflammation in the gut (77-79) and oxidative stress in the liver (80-82). However, whether the harmful effects of nPS could also be observed in HFD-fed mice remains elusive. Thus, histopathological examination was performed on the small intestine and liver samples. The F4/80 IHC staining in the small intestine showed a significant increase in macrophage infiltration following nPS treatment at both high and low dosages (Figures 7A, B). In addition, the H&E staining in liver samples showed more and

larger lipid droplets upon nPS treatment (Figure 7C), consistent with the TAG quantification results (Figure 7D). However, this pro-ectopic lipid accumulation function of nPS is not dose dependent. To further explore how nPS accelerated TAG level in the liver, we examined the mRNA level of the responsible genes. The nPS treatment increased the mRNA level of TAG synthetic gene (DGAT1) but did not induce the expression of key genes involved in de novo lipogenesis (FAS, SREBP-1c) or lipid droplet growth (Fsp27). In agreement with our results, acute i.v. injection of nPS (43 nm, 1 or 5 μg/mouse) also increased TAG accumulation and potentiated fibrosis in the liver in HFD fed female mice (42). In contrast, in the chow fed lean mouse model, oral exposure of NPs (500 nm at 200 μg/kg) for 5 weeks lowered lipid level in the liver (48) while 5 μm MP (100 μg/kg) for 4 weeks increased fat vacuoles in mice (82). The opposite effects of NPs in lipid metabolism in the liver from HFD and chow fed mice may be due to the basal metabolic status. When our mice were exposed to HFD and nPS simultaneously for 8 weeks, HFD induced more permeable gut barrier (74) and metabolic stress (83) in these mice. Therefore, the liver may be more susceptible to the exposure of nPS. Collectively, these data demonstrated a direct or indirect effect of nPS on ectopic lipid synthesis in the liver, however, the mechanism needs to be further studied.

## 4. Conclusion

In conclusion, we demonstrated that 60 nm-sized nPS preferentially accumulated in WAT and impaired lipid mobilization in adipocytes under stimulation both *in vitro* and *in vivo*, a result that was associated with the increased adipocyte size in subcutaneous WAT. Our work highlighted the potential obesogenic role of nPS via diminishing lipolytic response to β-adrenergic/fasting stimulation in WAT in obese mice for the first time. In addition, chronic oral exposure to nPS at the tested dosages increased inflammation in the gut and accelerated lipid accumulation in the liver in HFD-fed mice. Collectively, the results of this study demonstrated

the potential health risks of nPS in accelerating the development of obesity and its associated fatty liver diseases under HFD feeding conditions.

**Supplementary information:** Additional experimental materials and results as mentioned in the text

**Funding sources:** This work was supported, in part, by PolyU Internal Funding (#P0030234, #P0038706) and the Hong Kong Research Grants Council (Early Career Scheme #25100420) to Y.Z., and by PolyU Internal Funding (#P0001274) to James Kar-Hei Fang, and by the Collaborative Research Fund, Hong Kong Research Grants Council (# C5012-15E) to Ben Chi-Bun Ko.

**Notes:** The authors declare no competing financial interest.

**Acknowledgements:** We thank Dr. Wing-hin Kwok, Prof. Benjamin Yee and Dr. Wing-leung Wong for their insightful comments; Dr. Jiachi Chiou and Dr. Sai-wang Seto for sharing the technical insights; Dr. Yuen-Wa Ho for characterizing nPS with Raman; Mr. Kelvin Ching-Kwan Tsoi for quantifying nPS with Zetasizer; Dr. Vic Sun, Dr. Rachel Li and Dr. Michael Yuen for the technical support in mouse studies, IVIS imaging and confocal microscopy; Mr. Victor Ma and Mr Ho Yin Martin, Yeung for histological guidance. We thank the University Research Facility in Life Sciences (ULS) for providing equipment and technical support.

**Uncategorized References**

1. da Costa, J. P. *The 2019 global pandemic and plastic pollution prevention measures: Playing catch-up*, Sci Total Environ. 2021 Jun 20;774:145806. doi: 10.1016/j.scitotenv.2021.145806. Epub 2021 Feb 12.
2. Geyer, R., Jambeck, J. R., and Law, K. L. (2017) Production, use, and fate of all plastics ever made. *Sci Adv* **3**, e1700782
3. Evangeliou, N., Grythe, H., Kylling, A., and Stohl, A. (2021) Global emission, atmospheric transport and deposition trends of microplastics originating from road traffic. in *EGU General Assembly Conference Abstracts*
4. Benson, N. U., Bassey, D. E., and Palanisami, T. (2021) COVID pollution: impact of COVID-19 pandemic on global plastic waste footprint. *Heliyon* **7**, e06343

5. Peng, Y., Wu, P., Schartup, A. T., and Zhang, Y. (2021) Plastic waste release caused by COVID-19 and its fate in the global ocean. *Proc Natl Acad Sci U S A* **118**
6. Chamas, A., Moon, H., Zheng, J. J., Qiu, Y., Tabassum, T., Jang, J. H., Abu-Omar, M., Scott, S. L., and Suh, S. (2020) Degradation Rates of Plastics in the Environment. *Acs Sustain Chem Eng* **8**, 3494-3511
7. Hartmann, N. B., Nolte, T., Sørensen, M. A., Jensen, P. R., and Baun, A. (2015) Aquatic ecotoxicity testing of nanoplastics: lessons learned from nanoecotoxicology. *ASLO Aquatic Sciences Meeting* **Vol. 2015**
8. Gigault, J., Halle, A. T., Baudrimont, M., Pascal, P. Y., Gauffre, F., Phi, T. L., El Hadri, H., Grassl, B., and Reynaud, S. (2018) Current opinion: What is a nanoplastic? *Environ Pollut* **235**, 1030-1034
9. Hartmann, N. B., Huffer, T., Thompson, R. C., Hassellov, M., Verschoor, A., Daugaard, A. E., Rist, S., Karlsson, T., Brennholt, N., Cole, M., Herrling, M. P., Hess, M. C., Ivleva, N. P., Lusher, A. L., and Wagner, M. (2019) Are We Speaking the Same Language? Recommendations for a Definition and Categorization Framework for Plastic Debris. *Environ Sci Technol* **53**, 1039-1047
10. Alimba, C. G., and Faggio, C. (2019) Microplastics in the marine environment: Current trends in environmental pollution and mechanisms of toxicological profile. *Environ Toxicol Pharmacol* **68**, 61-74
11. Cox, K. D., Covernton, G. A., Davies, H. L., Dower, J. F., Juanes, F., and Dudas, S. E. (2019) Human Consumption of Microplastics. *Environ Sci Technol* **53**, 7068-7074
12. Wang, Y., Huang, J., Zhu, F., and Zhou, S. (2021) Airborne Microplastics: A Review on the Occurrence, Migration and Risks to Humans. *Bull Environ Contam Toxicol* **107**, 657-664
13. Koelmans, A. A., Mohamed Nor, N. H., Hermsen, E., Kooi, M., Mintenig, S. M., and De France, J. (2019) Microplastics in freshwaters and drinking water: Critical review and assessment of data quality. *Water Res* **155**, 410-422
14. Dawson, A. L., Kawaguchi, S., King, C. K., Townsend, K. A., King, R., Huston, W. M., and Bengtson Nash, S. M. (2018) Turning microplastics into nanoplastics through digestive fragmentation by Antarctic krill. *Nat Commun* **9**, 1001
15. Walczak, A. P., Hendriksen, P. J., Woutersen, R. A., van der Zande, M., Undas, A. K., Helsdingen, R., van den Berg, H. H., Rietjens, I. M., and Bouwmeester, H. (2015) Bioavailability and biodistribution of differently charged polystyrene nanoparticles upon oral exposure in rats. *Journal of Nanoparticle Research* **17**, 1-13
16. Florence, A. T., Hillery, A. M., Hussain, N., and Jani, P. U. (1995) Factors affecting the oral uptake and translocation of polystyrene nanoparticles: histological and analytical evidence. *J Drug Target* **3**, 65-70
17. Khan, I., Saeed, K., and Khan, I. (2019) Nanoparticles: Properties, applications and toxicities. *Arab J Chem* **12**, 908-931
18. Leslie, H. A., van Velzen, M. J. M., Brandsma, S. H., Vethaak, A. D., Garcia-Vallejo, J. J., and Lamoree, M. H. (2022) Discovery and quantification of plastic particle pollution in human blood. *Environ Int* **163**, 107199
19. Yong, C. Q. Y., Valiyaveetill, S., and Tang, B. L. (2020) Toxicity of Microplastics and Nanoplastics in Mammalian Systems. *Int J Environ Res Public Health* **17**
20. Qiao, R., Deng, Y., Zhang, S., Wolosker, M. B., Zhu, Q., Ren, H., and Zhang, Y. (2019) Accumulation of different shapes of microplastics initiates intestinal injury and gut microbiota dysbiosis in the gut of zebrafish. *Chemosphere* **236**, 124334
21. Gu, H., Wang, S., Wang, X., Yu, X., Hu, M., Huang, W., and Wang, Y. (2020) Nanoplastics impair the intestinal health of the juvenile large yellow croaker Larimichthys crocea. *J Hazard Mater* **397**, 122773

22. Lu, Y., Zhang, Y., Deng, Y., Jiang, W., Zhao, Y., Geng, J., Ding, L., and Ren, H. (2016) Uptake and Accumulation of Polystyrene Microplastics in Zebrafish (Danio rerio) and Toxic Effects in Liver. *Environ Sci Technol* **50**, 4054-4060
23. Wang, J., Li, Y., Lu, L., Zheng, M., Zhang, X., Tian, H., Wang, W., and Ru, S. (2019) Polystyrene microplastics cause tissue damages, sex-specific reproductive disruption and transgenerational effects in marine medaka (Oryzias melastigma). *Environ Pollut* **254**, 113024
24. Pitt, J. A., Trevisan, R., Massarsky, A., Kozal, J. S., Levin, E. D., and Di Giulio, R. T. (2018) Maternal transfer of nanoplastics to offspring in zebrafish (Danio rerio): A case study with nanopolystyrene. *Sci Total Environ* **643**, 324-334
25. Ding, J., Huang, Y., Liu, S., Zhang, S., Zou, H., Wang, Z., Zhu, W., and Geng, J. (2020) Toxicological effects of nano- and micro-polystyrene plastics on red tilapia: Are larger plastic particles more harmless? *J Hazard Mater* **396**, 122693
26. Yang, H., Xiong, H., Mi, K., Xue, W., Wei, W., and Zhang, Y. (2020) Toxicity comparison of nano-sized and micron-sized microplastics to Goldfish Carassius auratus Larvae. *J Hazard Mater* **388**, 122058
27. Marana, M. H., Poulsen, R., Thormar, E. A., Clausen, C. G., Thit, A., Mathiessen, H., Jaafar, R., Korbut, R., Hansen, A. M. B., Hansen, M., Limborg, M. T., Syberg, K., and von Gersdorff Jorgensen, L. (2022) Plastic nanoparticles cause mild inflammation, disrupt metabolic pathways, change the gut microbiota and affect reproduction in zebrafish: A full generation multi-omics study. *J Hazard Mater* **424**, 127705
28. Brandts, I., Balasch, J. C., Goncalves, A. P., Martins, M. A., Pereira, M. L., Tvarijonaviciute, A., Teles, M., and Oliveira, M. (2021) Immuno-modulatory effects of nanoplastics and humic acids in the European seabass (Dicentrarchus labrax). *J Hazard Mater* **414**, 125562
29. Pitt, J. A., Kozal, J. S., Jayasundara, N., Massarsky, A., Trevisan, R., Geitner, N., Wiesner, M., Levin, E. D., and Di Giulio, R. T. (2018) Uptake, tissue distribution, and toxicity of polystyrene nanoparticles in developing zebrafish (Danio rerio). *Aquat Toxicol* **194**, 185-194
30. Duan, Z., Duan, X., Zhao, S., Wang, X., Wang, J., Liu, Y., Peng, Y., Gong, Z., and Wang, L. (2020) Barrier function of zebrafish embryonic chorions against microplastics and nanoplastics and its impact on embryo development. *J Hazard Mater* **395**, 122621
31. da Costa Araujo, A. P., and Malafaia, G. (2021) Microplastic ingestion induces behavioral disorders in mice: A preliminary study on the trophic transfer effects via tadpoles and fish. *J Hazard Mater* **401**, 123263
32. Estrela, F. N., Guimaraes, A. T. B., Araujo, A., Silva, F. G., Luz, T. M. D., Silva, A. M., Pereira, P. S., and Malafaia, G. (2021) Toxicity of polystyrene nanoplastics and zinc oxide to mice. *Chemosphere* **271**, 129476
33. Prust, M., Meijer, J., and Westerink, R. H. S. (2020) The plastic brain: neurotoxicity of micro- and nanoplastics. *Part Fibre Toxicol* **17**, 24
34. Xu, D., Ma, Y., Han, X., and Chen, Y. (2021) Systematic toxicity evaluation of polystyrene nanoplastics on mice and molecular mechanism investigation about their internalization into Caco-2 cells. *J Hazard Mater* **417**, 126092
35. Yin, K., Wang, Y., Zhao, H., Wang, D., Guo, M., Mu, M., Liu, Y., Nie, X., Li, B., Li, J., and Xing, M. (2021) A comparative review of microplastics and nanoplastics: Toxicity hazards on digestive, reproductive and nervous system. *Science of The Total Environment* **774**, 145758
36. Gonzalez-Acedo, A., Garcia-Recio, E., Illescas-Montes, R., Ramos-Torrecillas, J., Melguizo-Rodriguez, L., and Costela-Ruiz, V. J. (2021) Evidence from in vitro and in vivo studies on the potential health repercussions of micro- and nanoplastics. *Chemosphere* **280**, 130826
37. Kannan, K., and Vimalkumar, K. (2021) A Review of Human Exposure to Microplastics and Insights Into Microplastics as Obesogens. *Front Endocrinol (Lausanne)* **12**, 724989

38. Lu, K., Lai, K. P., Stoeger, T., Ji, S., Lin, Z., Lin, X., Chan, T. F., Fang, J. K., Lo, M., Gao, L., Qiu, C., Chen, S., Chen, G., Li, L., and Wang, L. (2021) Detrimental effects of microplastic exposure on normal and asthmatic pulmonary physiology. *J Hazard Mater* **416**, 126069
39. Li, X., Zhang, T., Lv, W., Wang, H., Chen, H., Xu, Q., Cai, H., and Dai, J. (2022) Intratracheal administration of polystyrene microplastics induces pulmonary fibrosis by activating oxidative stress and Wnt/beta-catenin signaling pathway in mice. *Ecotoxicol Environ Saf* **232**, 113238
40. Jin, Y., Lu, L., Tu, W., Luo, T., and Fu, Z. (2019) Impacts of polystyrene microplastic on the gut barrier, microbiota and metabolism of mice. *Sci Total Environ* **649**, 308-317
41. Luo, T., Wang, C., Pan, Z., Jin, C., Fu, Z., and Jin, Y. (2019) Maternal Polystyrene Microplastic Exposure during Gestation and Lactation Altered Metabolic Homeostasis in the Dams and Their F1 and F2 Offspring. *Environ Sci Technol* **53**, 10978-10992
42. Li, L., Xu, M., He, C., Wang, H., and Hu, Q. (2021) Polystyrene nanoplastics potentiate the development of hepatic fibrosis in high fat diet fed mice. *Environ Toxicol*
43. Amereh, F., Babaei, M., Eslami, A., Fazelipour, S., and Rafiee, M. (2020) The emerging risk of exposure to nano(micro)plastics on endocrine disturbance and reproductive toxicity: From a hypothetical scenario to a global public health challenge. *Environ Pollut* **261**, 114158
44. Xie, X., Deng, T., Duan, J., Xie, J., Yuan, J., and Chen, M. (2020) Exposure to polystyrene microplastics causes reproductive toxicity through oxidative stress and activation of the p38 MAPK signaling pathway. *Ecotoxicol Environ Saf* **190**, 110133
45. Jeong, C. B., Won, E. J., Kang, H. M., Lee, M. C., Hwang, D. S., Hwang, U. K., Zhou, B., Souissi, S., Lee, S. J., and Lee, J. S. (2016) Microplastic Size-Dependent Toxicity, Oxidative Stress Induction, and p-JNK and p-p38 Activation in the Monogonont Rotifer (Brachionus koreanus). *Environ Sci Technol* **50**, 8849-8857
46. Rist, S., Baun, A., and Hartmann, N. B. (2017) Ingestion of micro- and nanoplastics in Daphnia magna - Quantification of body burdens and assessment of feeding rates and reproduction. *Environ Pollut* **228**, 398-407
47. Yin, L., Liu, H., Cui, H., Chen, B., Li, L., and Wu, F. (2019) Impacts of polystyrene microplastics on the behavior and metabolism in a marine demersal teleost, black rockfish (Sebastes schlegelii). *J Hazard Mater* **380**, 120861
48. Lu, L., Wan, Z., Luo, T., Fu, Z., and Jin, Y. (2018) Polystyrene microplastics induce gut microbiota dysbiosis and hepatic lipid metabolism disorder in mice. *Sci Total Environ* **631-632**, 449-458
49. Zhao, J., Gomes, D., Jin, L., Mathis, S. P., Li, X., Rouchka, E. C., Bodduluri, H., Conklin, D. J., and O'Toole, T. E. (2022) Polystyrene bead ingestion promotes adiposity and cardiometabolic disease in mice. *Ecotoxicol Environ Saf* **232**, 113239
50. Fan, X., Wei, X., Hu, H., Zhang, B., Yang, D., Du, H., Zhu, R., Sun, X., Oh, Y., and Gu, N. (2021) Effects of oral administration of polystyrene nanoplastics on plasma glucose metabolism in mice. *Chemosphere*, 132607
51. Zhang, W., Zhang, S., Wang, J., Wang, Y., Mu, J., Wang, P., Lin, X., and Ma, D. (2017) Microplastic pollution in the surface waters of the Bohai Sea, China. *Environ Pollut* **231**, 541-548
52. Hernandez, L. M., Xu, E. G., Larsson, H. C., Tahara, R., Maisuria, V. B., and Tufenkji, N. (2019) Plastic teabags release billions of microparticles and nanoparticles into tea. *Environmental science & technology* **53**, 12300-12310
53. Zhang, J., Wang, L., Trasande, L., and Kannan, K. (2021) Occurrence of Polyethylene Terephthalate and Polycarbonate Microplastics in Infant and Adult Feces. *Environmental Science & Technology Letters* **8**, 989-994
54. Lee, C.-H., and Fang, J. K.-H. (2022) Effects of temperature and particle concentration on aggregation of nanoplastics in freshwater and seawater. *Science of The Total Environment* **817**, 152562

55. Zhu, Y., Kim, S. Q., Zhang, Y., Liu, Q., and Kim, K. H. (2021) Pharmacological inhibition of acyl-coenzyme A:cholesterol acyltransferase alleviates obesity and insulin resistance in diet-induced obese mice by regulating food intake. *Metabolism* **123**, 154861
56. Williams, J. M., Duckworth, C. A., Vowell, K., Burkitt, M. D., and Pritchard, D. M. (2016) Intestinal Preparation Techniques for Histological Analysis in the Mouse. *Curr Protoc Mouse Biol* **6**, 148-168
57. Zhu, Y., Chen, C. Y., Li, J., Cheng, J. X., Jang, M., and Kim, K. H. (2018) In vitro exploration of ACAT contributions to lipid droplet formation during adipogenesis. *J Lipid Res* **59**, 820-829
58. Schweiger, M., Eichmann, T. O., Taschler, U., Zimmermann, R., Zechner, R., and Lass, A. (2014) Measurement of lipolysis. *Methods Enzymol* **538**, 171-193
59. Fournier, E., Etienne-Mesmin, L., Grootaert, C., Jelsbak, L., Syberg, K., Blanquet-Diot, S., and Mercier-Bonin, M. (2021) Microplastics in the human digestive environment: A focus on the potential and challenges facing in vitro gut model development. *J Hazard Mater* **415**, 125632
60. Ibrahim, Y. S., Tuan Anuar, S., Azmi, A. A., Wan Mohd Khalik, W. M. A., Lehata, S., Hamzah, S. R., Ismail, D., Ma, Z. F., Dzulkarnaen, A., Zakaria, Z., Mustaffa, N., Tuan Sharif, S. E., and Lee, Y. Y. (2021) Detection of microplastics in human colectomy specimens. *JGH Open* **5**, 116-121
61. Liu, L., Xu, K., Zhang, B., Ye, Y., Zhang, Q., and Jiang, W. (2021) Cellular internalization and release of polystyrene microplastics and nanoplastics. *Sci Total Environ* **779**, 146523
62. Cortés, C., Domenech, J., Salazar, M., Pastor, S., Marcos, R., and Hernández, A. (2020) Nanoplastics as a potential environmental health factor: effects of polystyrene nanoparticles on human intestinal epithelial Caco-2 cells. *Environmental Science: Nano* **7**, 272-285
63. DeLoid, G. M., Cao, X., Bitounis, D., Singh, D., Llopis, P. M., Buckley, B., and Demokritou, P. (2021) Toxicity, uptake, and nuclear translocation of ingested micro-nanoplastics in an in vitro model of the small intestinal epithelium. *Food and Chemical Toxicology* **158**, 112609
64. Im, G. B., Kim, Y. G., Jo, I. S., Yoo, T. Y., Kim, S. W., Park, H. S., Hyeon, T., Yi, G. R., and Bhang, S. H. (2022) Effect of polystyrene nanoplastics and their degraded forms on stem cell fate. *J Hazard Mater* **430**, 128411
65. Danopoulos, E., Twiddy, M., West, R., and Rotchell, J. M. (2022) A rapid review and meta-regression analyses of the toxicological impacts of microplastic exposure in human cells. *J Hazard Mater* **427**, 127861
66. Morigny, P., Boucher, J., Arner, P., and Langin, D. (2021) Lipid and glucose metabolism in white adipocytes: pathways, dysfunction and therapeutics. *Nat Rev Endocrinol* **17**, 276-295
67. Grabner, G. F., Xie, H., Schweiger, M., and Zechner, R. (2021) Lipolysis: cellular mechanisms for lipid mobilization from fat stores. *Nature metabolism* **3**, 1445-1465
68. Song, W., Popp, L., Yang, J., Kumar, A., Gangoli, V. S., and Segatori, L. (2015) The autophagic response to polystyrene nanoparticles is mediated by transcription factor EB and depends on surface charge. *J Nanobiotechnology* **13**, 87
69. Lim, S. L., Ng, C. T., Zou, L., Lu, Y., Chen, J., Bay, B. H., Shen, H. M., and Ong, C. N. (2019) Targeted metabolomics reveals differential biological effects of nanoplastics and nanoZnO in human lung cells. *Nanotoxicology* **13**, 1117-1132
70. Large, V., Reynisdottir, S., Langin, D., Fredby, K., Klannemark, M., Holm, C., and Arner, P. (1999) Decreased expression and function of adipocyte hormone-sensitive lipase in subcutaneous fat cells of obese subjects. *J Lipid Res* **40**, 2059-2066
71. U.S.Department of Health and Human Services, F., center for drug evaluation and research. (2005) Estimating the Maximum Safe Starting Dose in Initial Clinical Trials for Therapeutics in Adult Healthy Volunteers.
72. Luo, T., Zhang, Y., Wang, C., Wang, X., Zhou, J., Shen, M., Zhao, Y., Fu, Z., and Jin, Y. (2019) Maternal exposure to different sizes of polystyrene microplastics during gestation causes metabolic disorders in their offspring. *Environ Pollut* **255**, 113122

73. Martin, L. F., Klim, C. M., Vannucci, S. J., Dixon, L. B., Landis, J. R., and LaNoue, K. F. (1990) Alterations in adipocyte adenylate cyclase activity in morbidly obese and formerly morbidly obese humans. *Surgery* **108**, 228-234; discussion 234-225
74. Rohr, M. W., Narasimhulu, C. A., Rudeski-Rohr, T. A., and Parthasarathy, S. (2020) Negative Effects of a High-Fat Diet on Intestinal Permeability: A Review. *Adv Nutr* **11**, 77-91
75. Hou, J. K., Abraham, B., and El-Serag, H. (2011) Dietary intake and risk of developing inflammatory bowel disease: a systematic review of the literature. *Am J Gastroenterol* **106**, 563-573
76. Xu, Y. Y., Ge, J., Zhang, M. H., Sun, W. J., Zhang, J., Yu, P. L., Zheng, Y. F., Yang, J., and Zhu, X. Q. (2016) Intravenous Administration of Multiwalled Carbon Nanotubes Aggravates High-Fat Diet-Induced Nonalcoholic Steatohepatitis in Sprague Dawley Rats. *Int J Toxicol* **35**, 634-643
77. Li, B., Ding, Y., Cheng, X., Sheng, D., Xu, Z., Rong, Q., Wu, Y., Zhao, H., Ji, X., and Zhang, Y. (2020) Polyethylene microplastics affect the distribution of gut microbiota and inflammation development in mice. *Chemosphere* **244**, 125492
78. Deng, Y., Yan, Z., Shen, R., Wang, M., Huang, Y., Ren, H., Zhang, Y., and Lemos, B. (2020) Microplastics release phthalate esters and cause aggravated adverse effects in the mouse gut. *Environ Int* **143**, 105916
79. Hirt, N., and Body-Malapel, M. (2020) Immunotoxicity and intestinal effects of nano- and microplastics: a review of the literature. *Part Fibre Toxicol* **17**, 57
80. Deng, Y., Zhang, Y., Qiao, R., Bonilla, M. M., Yang, X., Ren, H., and Lemos, B. (2018) Evidence that microplastics aggravate the toxicity of organophosphorus flame retardants in mice (Mus musculus). *J Hazard Mater* **357**, 348-354
81. Deng, Y., Zhang, Y., Lemos, B., and Ren, H. (2017) Tissue accumulation of microplastics in mice and biomarker responses suggest widespread health risks of exposure. *Sci Rep* **7**, 46687
82. Zheng, H., Wang, J., Wei, X., Chang, L., and Liu, S. (2021) Proinflammatory properties and lipid disturbance of polystyrene microplastics in the livers of mice with acute colitis. *Sci Total Environ* **750**, 143085
83. Pang, J., Xi, C., Huang, X., Cui, J., Gong, H., and Zhang, T. (2016) Effects of Excess Energy Intake on Glucose and Lipid Metabolism in C57BL/6 Mice. *PLoS One* **11**, e0146675

## Figure legends:

**Figure 1. Characteristics of polystyrene nanoparticles (nPS).** (A) picture of fluorescent polystyrene particles by epi-fluorescent microscopy. (B) The spectrum of our nPS (in red) compared with the standard spectrum of PS (in green). (C) The size distribution of nPS dispersing in milliQ water measured by NanoSight.

**Figure 2. nPS preferentially accumulates in white adipose tissue in mice.** (A) IVIS images of the mice receiving fluorescent-nPS orally for four consecutive days (500 μg/day). (B) IVIS images of major organs of the mice in (A) to indicate the distribution of fluorescent-nPS. (C) Fluorescent-nPS signal was detected in the cryosections of perigonadal white adipose tissue from mice in (A).

**Figure 3. nPS shuttle across adipocytes in vitro but affect little on adipogenesis.** (A) 3T3-L1 preadipocytes and mature adipocytes were incubated with nPS at 37 °C or on ice for 8 hours. nPS-fluorescent signals were measured at the indicated time points (n = 3). (B) 3T3-L1 preadipocytes were cultured with nPS ($10^{10}$ particles/ml) during the whole period of adipogenesis, and the nuclei were stained with hoechst 33342. Three-D images were taken by confocal microscopy. White arrow points to the intranuclear green-nPS signal. (C) 3T3-L1 preadipocytes were differentiated in the presence or absence of nPS ($10^{10}$ particles/ml) from

days 0-6. Then adipocytes were cultured in serum free medium with or without isoproterenol to induce lipolysis, respectively. Intracellular fluorescent signals were quantified after 4 hours of lipolysis (n = 5). 3T3-L1 preadipocytes were differentiated with or without nPS at the indicated concentrations, representative images of Oil red O and the lipid quantifications are shown in (D) (n = 8). (E) Total RNA extracted from mature adipocytes was subjected to quantitative Realtime-PCR for the analysis of expression of genes involved in lipid synthesis (FAS, DGAT1, DGAT2). All data presented were mean ± S.E.M., *, $p < 0.05$; **, $p < 0.01$; ***, $p < 0.001$.

**Figure 4. nPS treatment impairs glycerol release upon lipolytic stimulation in adipocytes in vitro.** (A) Schematic diagram of lipolysis in adipocytes. (B) Adipocytes incubated with or without nPS (nPS and Ctrl groups, respectively) were cultured in low glucose medium in the presence or absence of isoproterenol (10 μM) for 1 and 2 hours, respectively. Associated mediums were collected to quantify free glycerol level as described in the experiments. (C) Epididymal WAT from eight-week-old C57BL/6J mice was minced and loaded with nPS, and the culture medium was collected after 6 hours' lipolysis in the presence or absence of isoproterenol as described in the experiment. Glycerol level was quantified in the medium.

**Figure 5. Chronic oral exposure to nPS had little effect on body or tissue weights.** (A) Schematic diagram of experimental design. Male C57BL/6J mice were given HFD and drinking water with or without nPS (3 and 223 μg/kg body weight/day, indicated as L-nPS and H-nPS, respectively) for 8 weeks. nPS treatment did not affect the body weight (B), food intake (C) or water intake (D) (n = 5 mice per group). The tissue weights of various organs [epididymal (Epi), Inguinal (Ing), retroperitoneal (Retro), mesenteric adipose tissue (MAT) and brown adipose tissue (BAT)] (E) were significantly higher in HFD-fed mice than those from chow diet fed age-matched mice. However, nPS treatment had little effect on the adipose tissue weight, spleen, pancreas, liver, or kidney (F, G). After 7 weeks of nPS-treatment, IPGTT was performed to measure mice glucose tolerance (H) and area of the curve (AOC) (I) of the IPGTT was calculated. (n = 5 mice per group). All data presented were mean ± S.E.M. *, $p < 0.05$; **, $p < 0.01$; ***, $p < 0.001$.

**Figure 6. Chronic oral exposure to nPS impaired fasting-induced lipolysis in obese mice.** The experimental mice in Figure 5 were overnight fasted and sacrificed as indicated in Figure 5A. Serum and several tissues were collected for further analysis: (A) The serum FFA levels were quantified (n = 5). (B) adipocyte size in inguinal WAT were quantified (n = 5). (C) Total RNA extracted from epiWAT was subjected to quantitative Realtime-PCR for the analysis of expression of genes involved in lipid synthesis (FAS, DGAT1, DGAT2) and adipokine (leptin). (D) Western blot analysis for ATGL, HSL, p-HSL and β-actin in epididymal WAT. Data are presented as means ± SEM. *, $p < 0.05$; **, $p < 0.01$; ***, $p < 0.001$. Unpaired Student's t-test was used for comparison between two groups.

**Figure 7. Chronic oral exposure to nPS accelerated lipid accumulation in liver.** (A) Representative images of F4/80 IHC-stained small intestine sections from ctrl and nPS treatment groups. (B) The number of macrophages on the small intestine samples showed a dose-dependent increase. (C) Representative images of H&E-stained liver sections from ctrl and nPS treatment. Scale bar is 50 μm. (D) Liver triglyceride level was measured in Ctrl and nPS treatment mice (n = 5). (E) qRT-PCR analysis of lipogenic genes in liver samples (n = 4). All data presented were mean ± S.E.M. *, $p < 0.05$; **, $p < 0.01$; ***, $p < 0.001$.

Click here to access/download;Figure;Figure and legends 20220615 (R1).docx

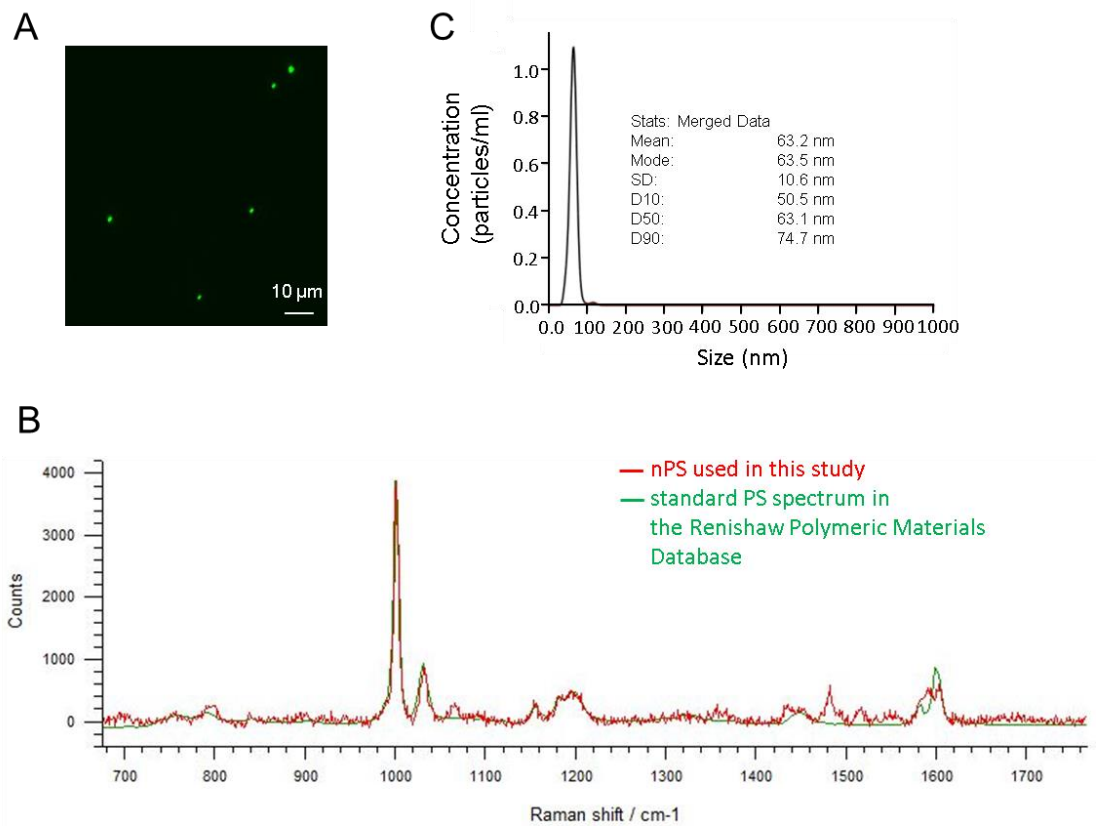


**Figure 1. Characteristics of polystyrene nanoparticles (nPS).** (A) picture of fluorescent polystyrene particles by epi-fluorescent microscopy. (B) The spectrum of our nPS (in red) compared with the standard spectrum of PS (in green). (C) The size distribution of nPS dispersing in milliQ water measured by NanoSight.

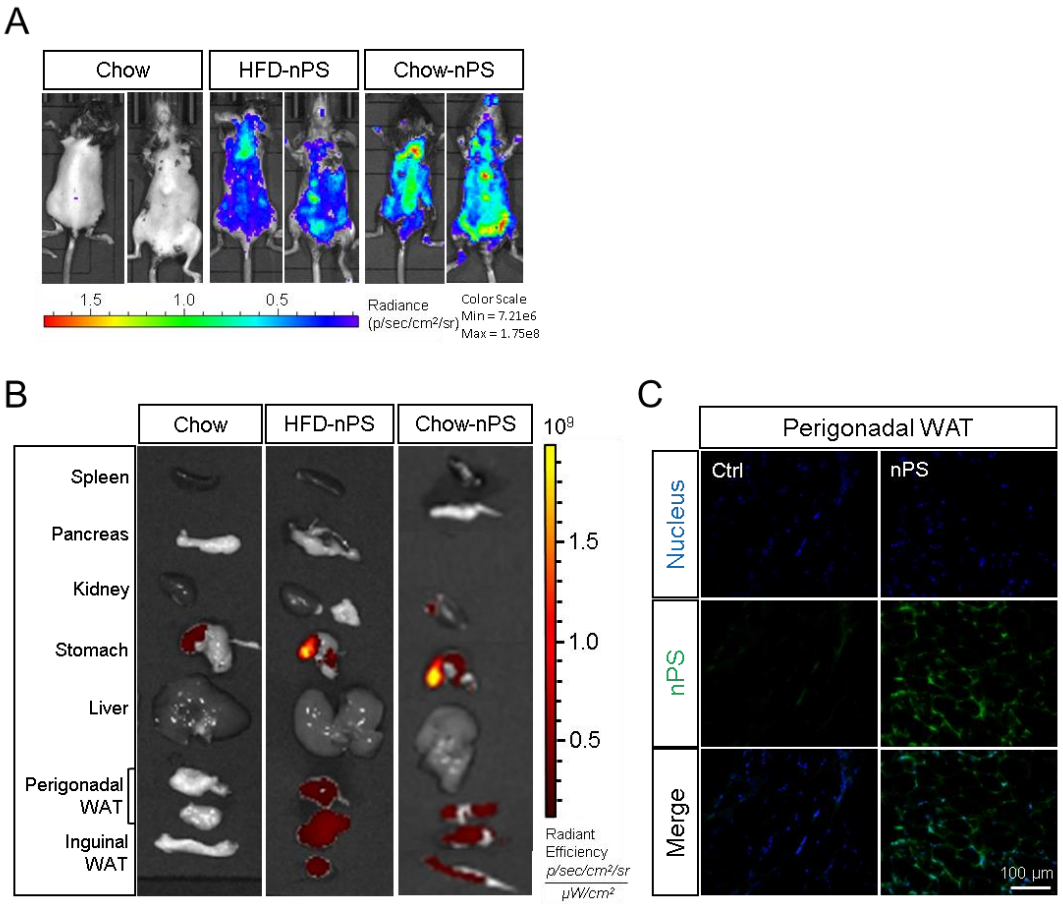


**Figure 2. nPS preferentially accumulates in white adipose tissue in mice.** (A) IVIS images of the mice receiving fluorescent-nPS orally for four consecutive days (500 μg/day). (B) IVIS images of major organs of the mice in (A) to indicate the distribution of fluorescent-nPS. (C) Fluorescent-nPS signal was detected in the cryosections of perigonadal white adipose tissue from mice in (A).

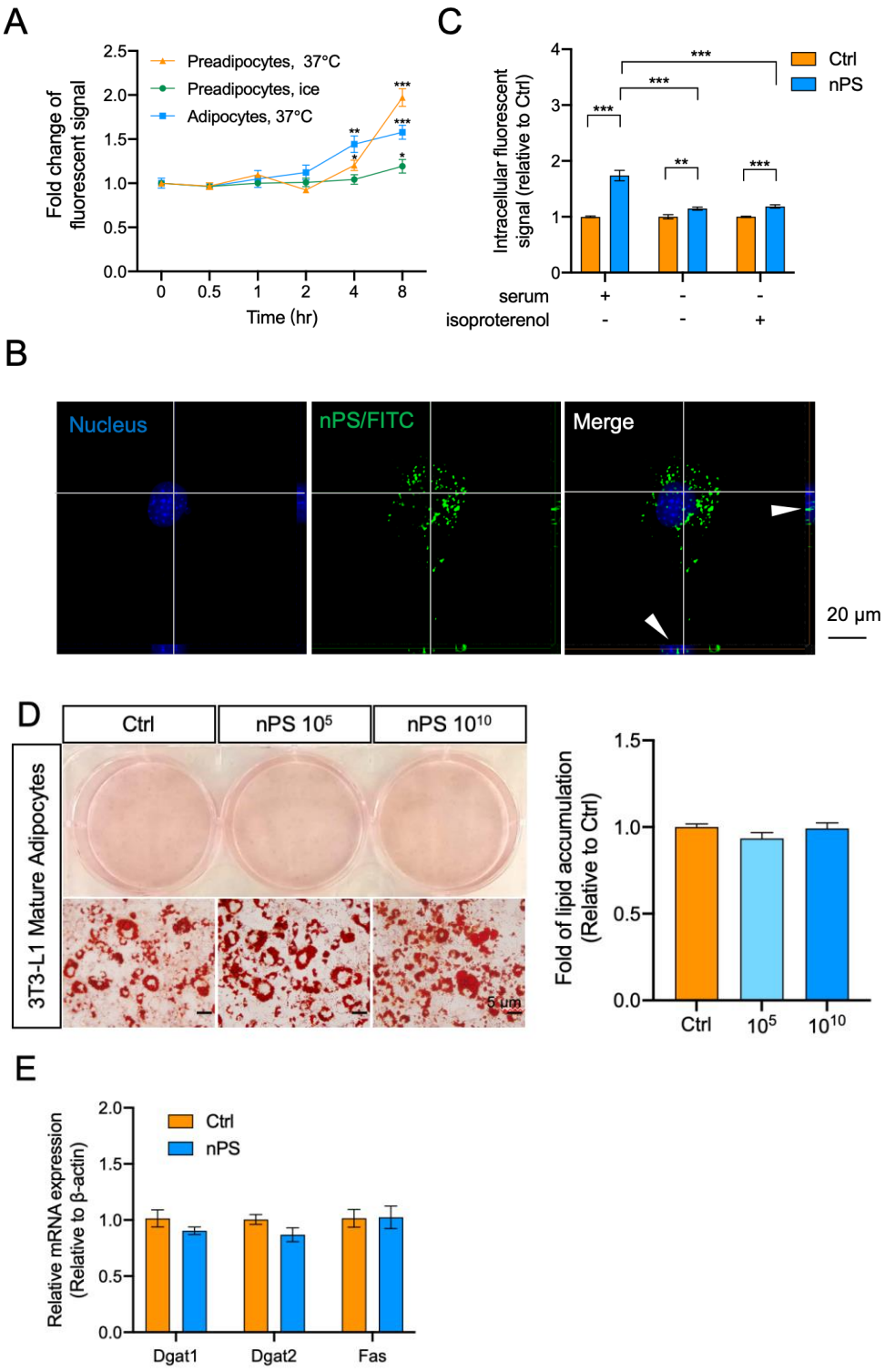


**Figure 3. nPS shuttle across adipocytes in vitro but affect little on adipogenesis.** (A) 3T3-L1 preadipocytes and mature adipocytes were incubated with nPS at 37 °C or on ice for 8 hours. nPS-fluorescent signals were measured at the indicated time points (n = 3). (B) 3T3-L1 preadipocytes were cultured with nPS ($10^{10}$ particles/ml) during the whole period of adipogenesis, and the nuclei were stained with hoechst 33342. Three-D images were taken by confocal microscopy. White arrow points to the intranuclear

green-nPS signal. (C) 3T3-L1 preadipocytes were differentiated in the presence or absence of nPS ($10^{10}$ particles/ml) from days 0-6. Then adipocytes were cultured in serum free medium with or without isoproterenol to induce lipolysis, respectively. Intracellular fluorescent signals were quantified after 4 hours of lipolysis (n = 5). 3T3-L1 preadipocytes were differentiated with or without nPS at the indicated concentrations, representative images of Oil red O and the lipid quantifications are shown in (D) (n = 8). (E) Total RNA extracted from mature adipocytes was subjected to quantitative Realtime-PCR for the analysis of expression of genes involved in lipid synthesis (FAS, DGAT1, DGAT2). All data presented were mean ± S.E.M., *, $p < 0.05$; **, $p < 0.01$; ***, $p < 0.001$.

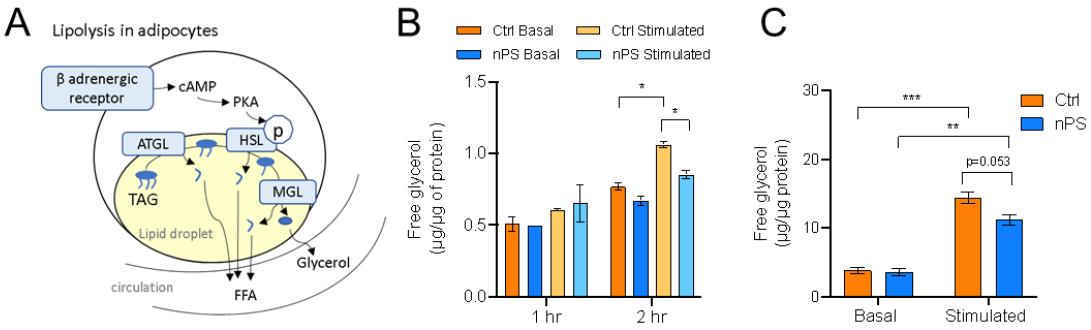


**Figure 4. nPS treatment impairs glycerol release upon lipolytic stimulation in adipocytes in vitro.** (A) Schematic diagram of lipolysis in adipocytes. (B) Adipocytes incubated with or without nPS (nPS and Ctrl groups, respectively) were cultured in low glucose medium in the presence or absence of isoproterenol (10 μM) for 1 and 2 hours, respectively. Associated mediums were collected to quantify free glycerol level as described in the experiments. (C) Epididymal WAT from eight-week-old C57BL/6J mice was minced and loaded with nPS, and the culture medium was collected after 6 hours' lipolysis in the presence or absence of isoproterenol as described in the experiment. Glycerol level was quantified in the medium.

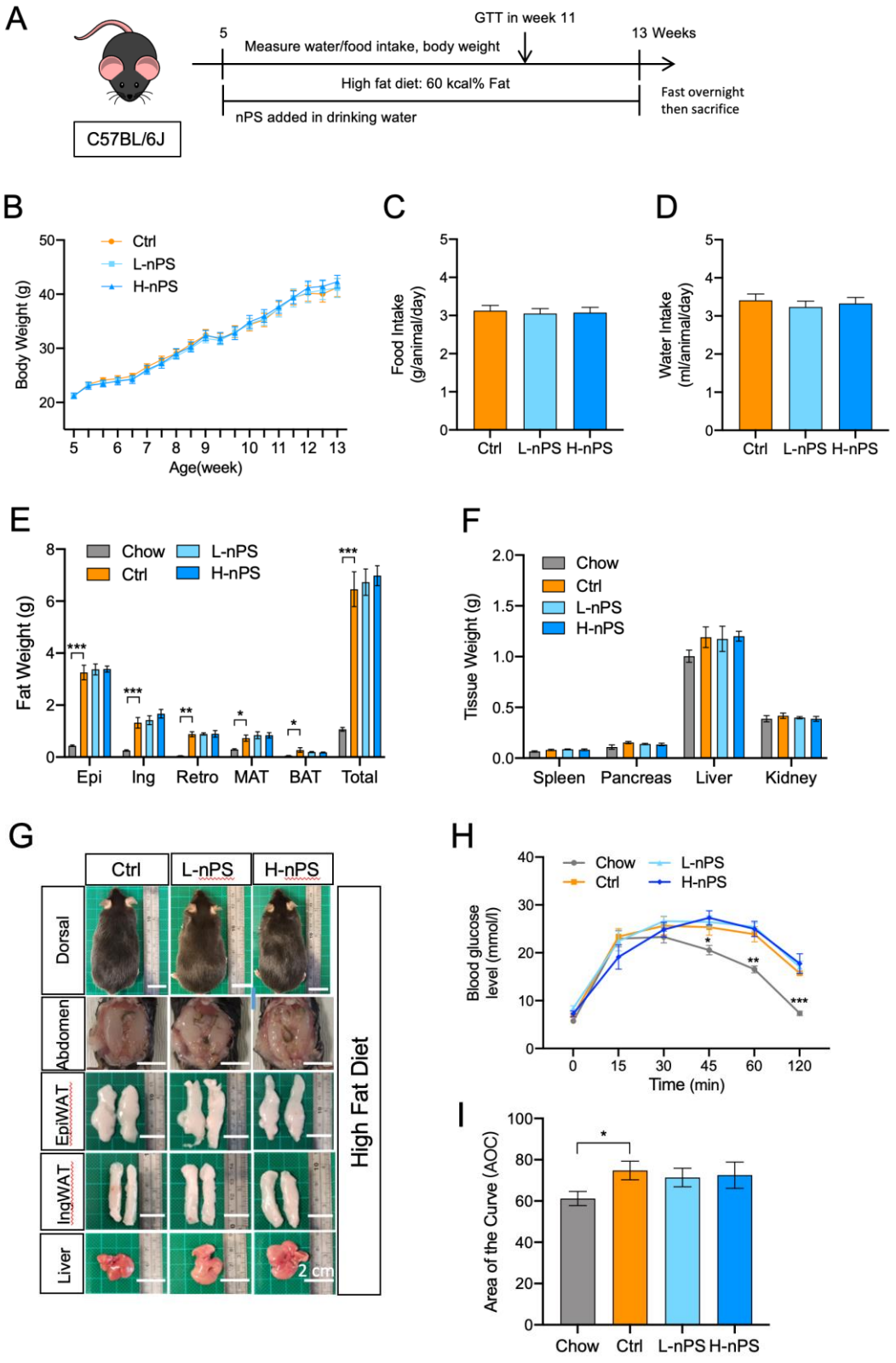


**Figure 5. Chronic oral exposure to nPS had little effect on body or tissue weights.** (A) Schematic diagram of experimental design. Male C57BL/6J mice were given HFD and drinking water with or without nPS (3 and 223 μg/kg body weight/day, indicated as L-nPS

and H-nPS, respectively) for 8 weeks. nPS treatment did not affect the body weight (B), food intake (C) or water intake (D) (n = 5 mice per group). The tissue weights of various organs [epididymal (Epi), Inguinal (Ing), retroperitoneal (Retro), mesenteric adipose tissue (MAT) and brown adipose tissue (BAT)] (E) were significantly higher in HFD-fed mice than those from chow diet fed age-matched mice. However, nPS treatment had little effect on the adipose tissue weight, spleen, pancreas, liver, or kidney (F, G). After 7 weeks of nPS-treatment, IPGTT was performed to measure mice glucose tolerance (H) and area of the curve (AOC) (I) of the IPGTT was calculated. (n = 5 mice per group). All data presented were mean ± S.E.M. *, $p < 0.05$; **, $p < 0.01$; ***, $p < 0.001$.

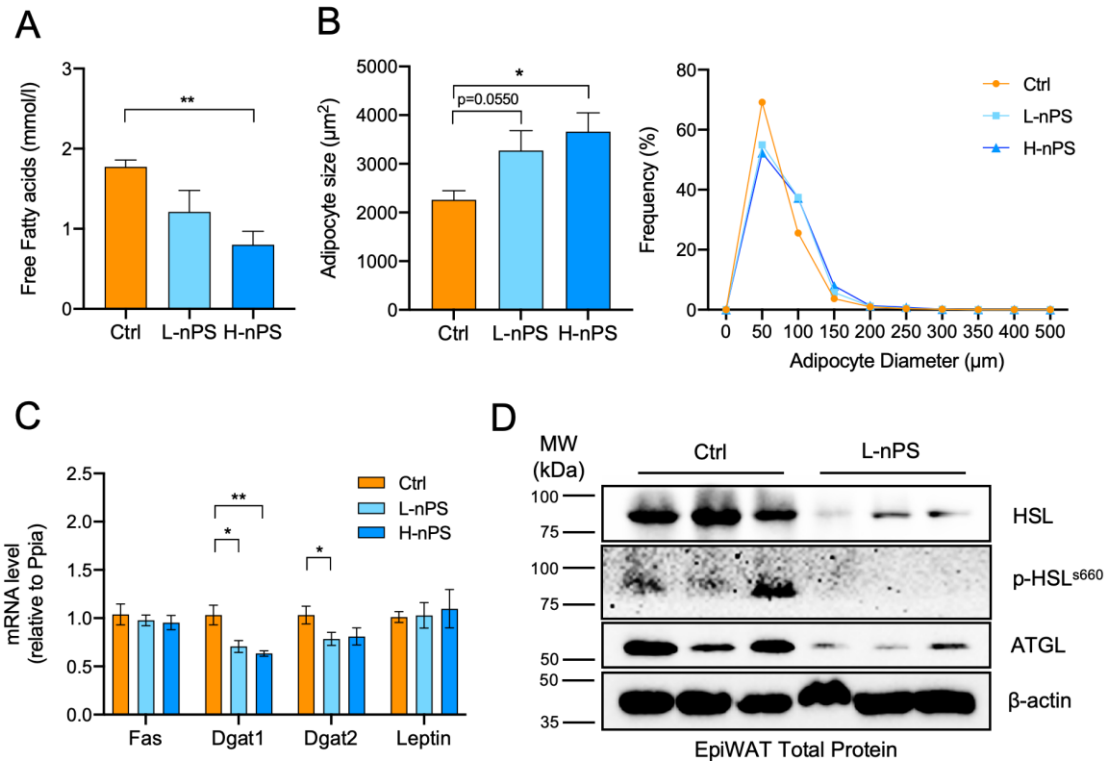


**Figure 6. Chronic oral exposure to nPS impaired fasting-induced lipolysis in obese mice.**

The experimental mice in Figure 5 were overnight fasted and sacrificed as indicated in

Figure 5A. Serum and several tissues were collected for further analysis: (A) The serum FFA levels were quantified (n = 5). (B) adipocyte size in inguinal WAT were quantified (n = 5). (C) Total RNA extracted from epiWAT was subjected to quantitative Realtime-PCR for the analysis of expression of genes involved in lipid synthesis (FAS, DGAT1, DGAT2) and adipokine (leptin). (D) Western blot analysis for ATGL, HSL, p-HSL and β-actin in epididymal WAT. Data are presented as means ± SEM. *, $p < 0.05$; **, $p < 0.01$; ***, $p < 0.001$. Unpaired Student's t-test was used for comparison between two groups.

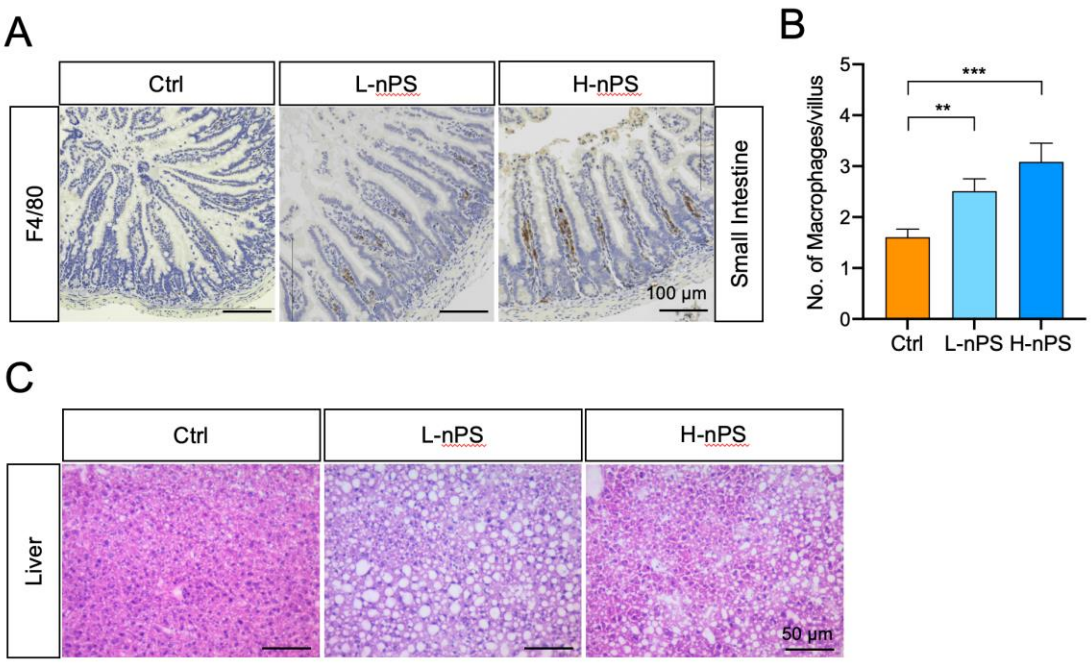

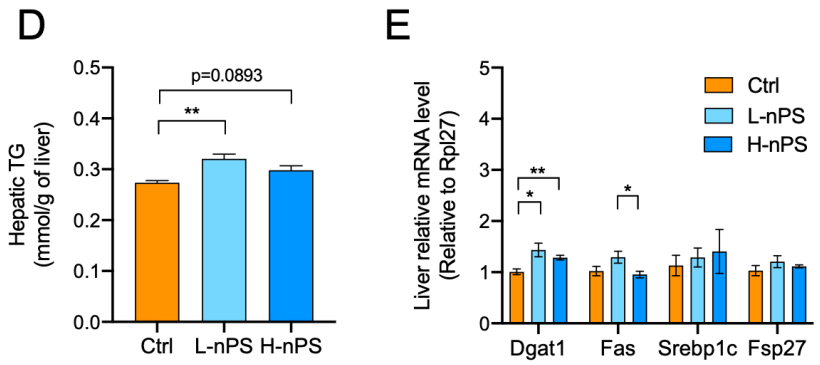


**Figure 7. Chronic oral exposure to nPS accelerated lipid accumulation in liver.** (A) Representative images of F4/80 IHC-stained small intestine sections from ctrl and nPS treatment groups. (B) The number of macrophages on the small intestine samples showed a dose-dependent increase. (C) Representative images of H&E-stained liver sections from ctrl and nPS treatment. Scale bar is 50 μm. (D) Liver triglyceride level was measured in Ctrl and nPS treatment mice (n = 5). (E) qRT-PCR analysis of lipogenic genes in liver samples (n = 4). All data presented were mean ± S.E.M. *, $p < 0.05$; **, $p < 0.01$; ***, $p < 0.001$.

Click here to access/download
**Supplementary Material**
Supplementary material 20220722 (R2).docx

**CRediT author statement**

**Ho Ting Shiu:** Methodology, Formal analysis, Investigation, Writing-Original draft preparation; **Xiaohan Pan**: Methodology, Formal analysis, Investigation, Writing-Original draft preparation; **Qing Liu:** Methodology, Formal analysis, Investigation; **KeKao Long:** Methodology; **Kenneth King Yip Cheng:** Methodology; **Ben Chi-Bun Ko**: Methodology; **James Kar-Hei Fang:** Methodology, Formal analysis; **Yuyan Zhu**: Methodology, Formal analysis, Supervision, Writing – original draft, Validation.

**Declaration of interests**

☒The authors declare that they have no known competing financial interests or personal relationships that could have appeared to influence the work reported in this paper.

☐The authors declare the following financial interests/personal relationships which may be considered as potential competing interests: